GEM-QUALITY AUGITE FROM DONG NAI, VIETNAM

Le Ngoc Nang, Lam Vinh Phat, Pham Minh Tien, Pham Trung Hieu, Kenta Kawaguchi, and Pham Minh

Augite from Dong Nai Province in Vietnam occurs as xenocrysts hosted by Cenozoic basalt and its regolith. Found as irregularly shaped crystals a few millimeters to centimeters in size, these augites exhibit two dominant colors: brown and green. They are very dark in tone, making them appear almost black in reflected light and are translucent to transparent, with vitreous luster. Most of the samples' gemological properties are similar except for refractive index and birefringence values, which are both higher in green augite. The brown and green augite samples show differences in Raman peak positions. The chemical composition as determined by electron probe microanalysis suggests that Dong Nai augite should be classified as magnesium-rich augite. This material is promising for jewelry use, as gem-quality material is readily found over a large area.

Augite is a monoclinic member of the pyroxene group [(M2)(M1)$(T)_2O_6$] with the general formula $(Ca,Na)(Mg,Fe,Al,Ti)(Si,Al)_2O_6$ (Morimoto, 1989), where M1 and M2 are octahedrally coordinated cation sites and T is a tetrahedrally coordinated cation site. Augite is most commonly found in mafic igneous rocks such as basalts and gabbros, as well as in ultramafic rocks (Anthony et al., 2001). The pyroxene group includes a wide range of well-known and highly valuable gem varieties used in jewelry, including jadeite ($NaAlSi_2O_6$), spodumene ($LiAlSi_2O_6$), diopside ($CaMgSi_2O_6$), and omphacite ($(Ca,Na)(Mg, Fe^{2+},Al)Si_2O_6$) (Mei et al., 2003; O'Donoghue et al., 2006). However, augite is generally not considered a gem material because most examples are opaque, with unattractive colors (Hurwit, 1988; Johnson et al., 1996).

In 2018, two types of gem-quality augite appeared in the Ho Chi Minh City marketplace: dark green and dark orangy brown (figure 1). All of these were loose stones (faceted, cabochon cut, or carved). The gems appeared black in reflected light, but color could be seen in transmitted light. One dealer noted that they were mined in Dong Nai Province and initially mistaken for diopside and tourmaline. The samples were later submitted to Liu Gemological Research and Application Center (LIULAB) and identified as augite.

After learning of this potential source of gem-quality augite, the authors decided to visit the deposit. We began our study in the center of Dong Nai Province (figure 2), where we collected a large quantity of gem-quality samples during two field trips in May 2020 and October 2021. The augite occurred as xenocrysts hosted by basalt bedrock, which was covered by a regolith layer of basaltic laterite. This paper aims to identify the variety of augite from Dong Nai and describe its formation and gemological characteristics.

In Brief

- An abundant source of xenocrystic gem-quality augite was discovered in an alkali basalt formation in Dong Nai, Vietnam.
- Dark green and dark brown are the two color varieties of this augite; except for RI, their gemological properties are similar.
- Raman spectroscopy helps differentiate the two varieties of augite and distinguish between green augite and diopside.
- Augite from Dong Nai is suitable for fashioning in faceted, cabochon, and especially carved form.

GEOLOGICAL SETTING

The augite deposit is located in the center of Gia Kiem commune in the Thong Nhat district of Dong Nai Province (figure 3) in the southeast region of

See end of article for About the Authors and Acknowledgments.
GEMS & GEMOLOGY, Vol. 59, No. 2, pp. 182–194,
http://dx.doi.org/10.5741/GEMS.59.2.182

Figure 1. The deep colors of green and brown augite from Dong Nai, observed in transmitted light. Top: The 9.78 g rough on the left yielded a 24.20 ct carving (24.99 mm in height). Bottom: The 11.22 g rough on the left yielded a 56.10 ct carving (36.50 mm in height). Photos by Le Ngoc Nang.

Vietnam, about 90 km north of Ho Chi Minh City. In May 2020 and October 2021, we conducted field trips to this area to collect samples and investigate the site. The sampling site is in the midland, a tran-

Figure 2. View of a valley in Dong Nai, Vietnam, where vegetation grows on the topsoil of the augite-bearing basaltic regolith. Photo by Lam Vinh Phat.

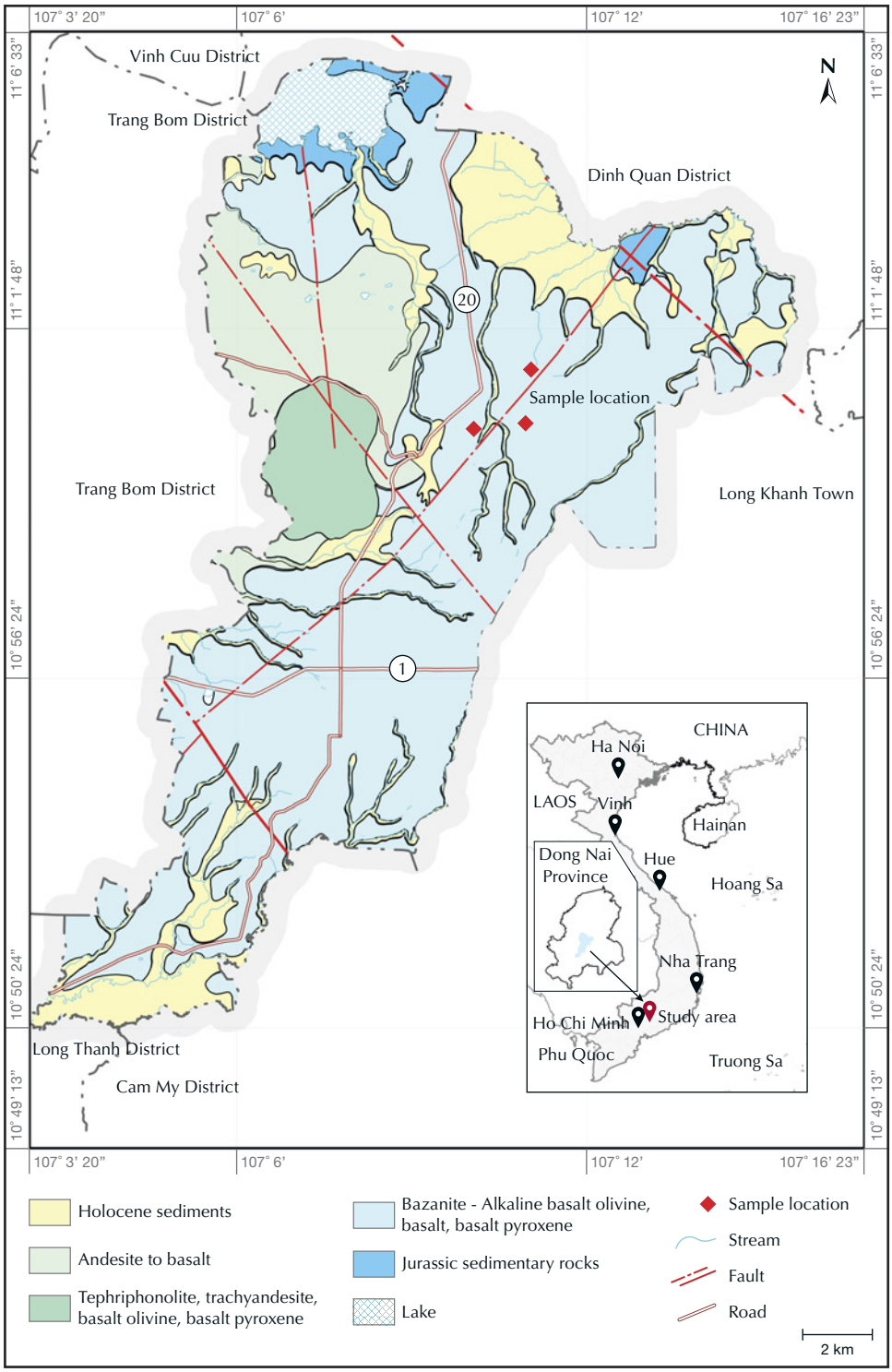

Figure 3. The augite occurrence is hosted by a Cenozoic basaltic formation and Quaternary sediments along the stream in the valley. Modified from Son et al. (2005).

sition zone between the plains and the highlands. From the north, the terrain descends gradually toward the south, and temporary streams and springs carve through rolling hills. The average elevation is about 139 m above mean sea level, with the slope steepness varying from 30° to 80°. Landforms include a plain of denudation and cinder cones (Son et al., 2005; Bac and Bao, 2020). The plain of denudation occurs on Jurassic sedimentary rock, with the erosion surface dating to the Late Pliocene to Early Pleistocene, before the eruption of the basaltic lava that covers almost the entire erosion surface (Bac and Bao,

Figure 4. Augite is abundant in Dong Nai Province and easy to collect. A: Augite hosted by basalt. B: Augite buried in laterite soil. C: Samples obtained during the field trips, which appear black under reflected light before revealing an orangy brown or a green color when observed in transmitted light. Photos by Lam Vinh Phat.

2020). The study location in Dong Nai is centered on a dormant volcano zone that was active during the period from the Neogene to the Quaternary (Bac and Bao, 2020) (again, see figure 3). The regolith is quite thick, containing mostly red and gray soils and sometimes basaltic boulders. Due to the area's tropical climate, mechanical weathering also causes exfoliation on most of the bedrock.

Dong Nai augite xenocrysts are found in basalt and its laterite (figure 4). In the mid-Pleistocene, the xenocryst-bearing basalt formed by volcanic eruption, resulting in a 70–200 m high terrain covering a large area. The augite-bearing basalt is dark bluish gray and light to dark gray and consists mainly of alkaline olivine (Co and Hai, 1994; Son et al., 2005; Bac and Bao, 2020). The xenocryst-bearing basalt is of vesicular structure with a void ratio varying from 3% to 15% with round, oval, and sometimes irregular shapes. The average void size ranges from 0.5 × 1.0 mm to 4.0 × 8.0 mm. In addition to pyroxene, other rock-forming minerals such as feldspar and clusters of olivine are contained sparsely in the basalt, with xenocrysts ranging in size from 0.5 to 10.0 cm and clusters of olivine from 2 to 15 cm (1–2 mm per crystal) (Son et al., 2005; Bac and Bao, 2020).

At a height of approximately 120 m above mean sea level, the augite-bearing basalt is weathered to varying degrees into brown to yellowish brown regolith. The regolith is moderately thick, about 2–3 m. The weathering profile contains the saprolite and the saprock of weathered basalt overlain by topsoil (Son et al., 2005).

During land reclamation since 2019, farmers in Dong Nai have been collecting the augite by hand and shovel. No mining activity takes place in this area. The authors connected with three merchants who gather and cut these augites for sale as tourmaline or diopside. These merchants gather 120 kg of gem-quality augite annually from the farmers and own 20,000 carats of faceted material, none of which is exported. Their current consumer market is limited to Ho Chi Minh City and some Vietnamese provinces.

Figure 5. Augite samples from this study were fashioned as faceted gems, cabochons, and carvings. These are shown in reflected light (first and third rows) and transmitted light (second and fourth rows). Photos by Le Ngoc Nang.

MATERIALS AND METHODS

Samples. During the two field trips, we collected more than 100 samples ranging from 2.4 to 100 g (figure 4C). We selected a total of 16 clear transparent to translucent samples (eight green and eight brown) for standard gemological testing as well as powder X-ray diffraction (XRD) and electron probe microanalysis (EPMA). We had 12 samples cut from the rough (figure 5). These samples included six faceted pieces (brown samples A1, A2, and A3; green samples A7, A8, and A9); four flat-bottom cabochons (brown samples A4 and A5; green samples A10 and A11); and two carved pieces (brown sample A6; green sample A12). All the faceted and cabochon samples were cut at a lapidary facility in Ho Chi Minh City, and the rest were carved by a freelance gem cutter in Ho Chi Minh City. We used the six faceted gems to analyze the Raman and Fourier-transform infrared spectra. Two other samples, a 15.56 ct transparent brown sample (A13) and a 12.08 ct transparent green sample (A14), had their surface impurities removed by a lapidary machine before being ground for powder XRD analysis (figure 6). Lastly, a 34.36 ct brown sample (A15) and a 41.20 ct green sample (A16) were ground into thin sections for EPMA measurement (figure 6).

Standard Gemological Methods. Standard gemological testing was performed on the fashioned augite samples (A1–A12) at LIULAB to determine their refractive index (RI), hydrostatic specific gravity (SG), and fluorescence reaction to long-wave (365 nm) and short-wave (254 nm) UV light. Optical properties and pleochroism were observed with a polariscope and dichroscope, respectively. The physical appearance was documented using fiber-optic lighting, both ambient and transmitted using a 60W GLS LED daylight bulb with a temperature of approximately 5000–6000K. For ambient lighting the settings were 8 volts and 10 watts, and for transmitted lighting the settings were 8 volts and 20 watts. Microscopic features were viewed using a Carton 7×–50× gemological microscope.

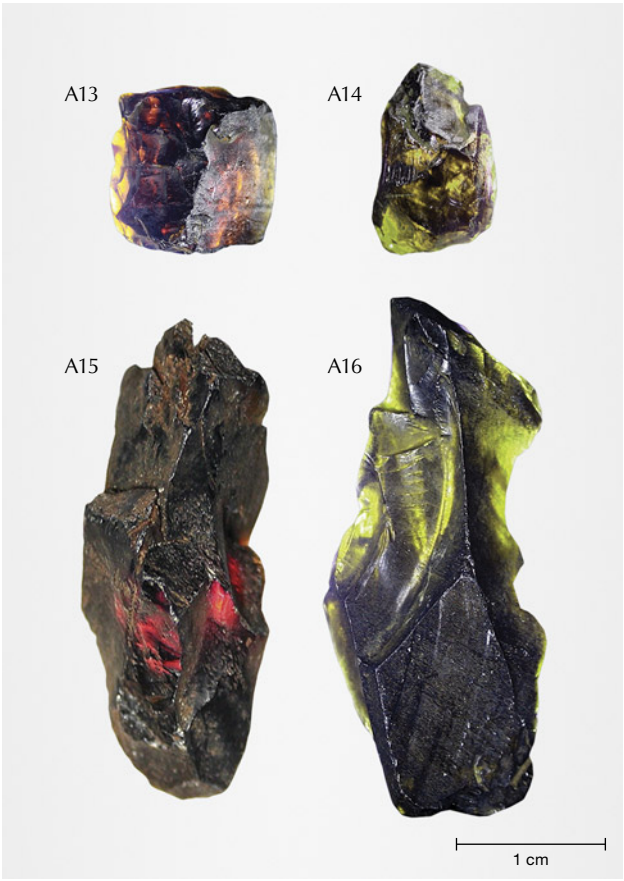

Figure 6. Rough augite samples before grinding and polishing for XRD (A13 and A14) and EPMA (A15 and A16), shown in transmitted light. Photos by Pham Minh Tien.

Analytical Methods. EPMA was performed on samples A15 (brown) and A16 (green) using a JEOL JXA-8200 instrument. Analyses were obtained with an electron probe diameter of 3 µm, an accelerating voltage of 15 kV, and a beam current of 20 nA, following the methods of Kawaguchi et al. (2022). Measurements of the oxides SiO_2, TiO_2, Al_2O_3, FeO, Cr_2O_3, MnO, CaO, Na_2O, K_2O, MgO, and P_2O_5 were obtained to determine the variety of pyroxene (Lindsley, 1983; Morimoto, 1989). The calibration standards included quartz for silicon, corundum for aluminum, manganosite for manganese, periclase for magnesium, nickel oxide for nickel, fayalite for iron, wollastonite for calcium, jadeite for sodium, and potassium titanium phosphate for potassium.

XRD is a common technique used to identify a mineral based on the scattering of X-rays by the atoms in a crystal structure. The diffraction patterns were collected by a Bruker D2 Phaser powder XRD, using CuKα (1.5406 Å) radiation in the range of 5–75° 2θ with a scan speed of 0.02°/s, at 40 kV and 30 mA. Brown sample A13 and green sample A14 were ground to a particle size of 5 µm. We used X'Pert HighScore software to analyze the results and compare them to the standard data in the Inorganic Crystal Structure Database (ICSD).

Raman spectroscopy was performed using a Horiba Xplora One Raman confocal microscope in the range of 0 to 3750 cm^{-1} with three brown samples (A1, A2, and A3) and three green samples (A7, A8, and A9). Measurements were performed at a laser excitation wavelength of 532 nm, laser mode power at 50%, and a 900 lines/mm diffraction grating, with a spectral resolution of 5 cm^{-1}. The objective selected was of 50× magnification. Raman spectra were collected over 15 s with two signal accumulations.

X-ray diffraction and Raman spectroscopy were conducted at the Institute of Chemical Technology, Vietnam Academy of Science and Technology. EPMA was performed at Hiroshima University in Japan.

RESULTS AND DISCUSSION

Appearance. The fabricated augite samples from Dong Nai were transparent to translucent, with vitreous luster. All of them appeared black under daylight-equivalent lighting. When observed in transmitted light, they displayed one of two colors: dark green or dark orangy brown.

Augite generally receives little attention in the jewelry industry because of its very dark appearance (see video at https://www.gia.edu/gems-gemology/summer-2023-augite-from-vietnam). Dong Nai augite appears homogenously black and opaque in reflected light but transparent and dark green, or orangy brown, when viewed in transmitted light. Moreover, a low degree of fracturing with massive form allows Dong Nai augite to be well polished and fashioned, particularly as carvings and cabochons (figures 1 and 5). After evaluating these features on the specimens processed from our samples, we concluded that augite from Dong Nai has potential application in the jewelry industry.

Gemological Properties and Identification. The gemological properties of the Dong Nai augite samples are described and summarized in table 1. Specific gravity values ranged from 3.36 to 3.38. The RI values measured for the five brown samples were n_p 1.674–1.676 and n_g 1.685–1.686, for a birefringence Δn of 0.009–0.012. RI values for the five green specimens were n_p 1.683–1.688 and n_g 1.703–1.706, for a

TABLE 1. Gemological properties of 16 augite samples from Dong Nai, Vietnam.

Sample no.	Weight (ct)	Color[a]	Form	SG	RI		Birefringence	Pleochroism
					n_p	n_g		
A1	4.60	Dark orangy brown	Faceted square	3.36	1.674	1.686	0.012	Brown to black
A2	4.97	Dark orangy brown	Faceted oval	3.34	1.672	1.682	0.010	Brown to black
A3	10.08	Dark orangy brown	Faceted oval	3.37	1.675	1.685	0.010	Greenish brown to black
A4	12.70	Dark orangy brown	Oval cabochon	3.34	1.673	1.685	0.012	Brown to black
A5	8.51	Dark orangy brown	Oval cabochon	3.36	1.672	1.682	0.010	Brown to black
A6	31.55	Dark orangy brown	Carving	3.35	1.67[b]		na[c]	Deep green to black
A7	12.65	Dark green	Faceted oval	3.37	1.685	1.705	0.020	Deep green to black
A8	7.28	Dark green	Faceted round	3.37	1.686	1.702	0.016	Deep green to black
A9	3.89	Dark green	Faceted rectangle	3.35	1.685	1.702	0.017	Deep green to black
A10	12.53	Dark green	Oval cabochon	3.36	1.688	1.703	0.015	Deep green to black
A11	9.59	Dark green	Oval cabochon	3.34	1.688	1.705	0.017	Deep green to black
A12	14.18	Dark green	Carving	3.35	1.70[b]		na	Deep green to black
A13	15.56	Dark orangy brown	Rough	3.33	—	—	na	Brown to black
A14	12.08	Dark green	Rough	3.35	—	—	na	Deep green to black
A15	34.36	Dark orangy brown	Rough	3.35	—	—	na	Brown to black
A16	41.20	Dark green	Rough	3.36	—	—	na	Deep green to black

[a]*Observed in transmitted light*
[b]*Spot RI*
[c]*na = not analyzed*

birefringence of 0.016–0.020. The RI values measured by spot reading method of two carved samples (A6 and A12) were 1.67 and 1.70. All samples were biaxial when viewed with a polariscope. None of them reacted to either long-wave or short-wave UV light. When viewed with a dichroscope, the green samples showed strong pleochroism from deep green to black (table 1), while the brown stones showed brown to black. The Mohs hardness of the rough samples was about 5–6. All of these gemological properties were consistent with augite (Manutchehr-Danai, 2005).

The gemological properties of the green and brown gems were similar except for RI and birefringence, which were higher for the green group (table 1).

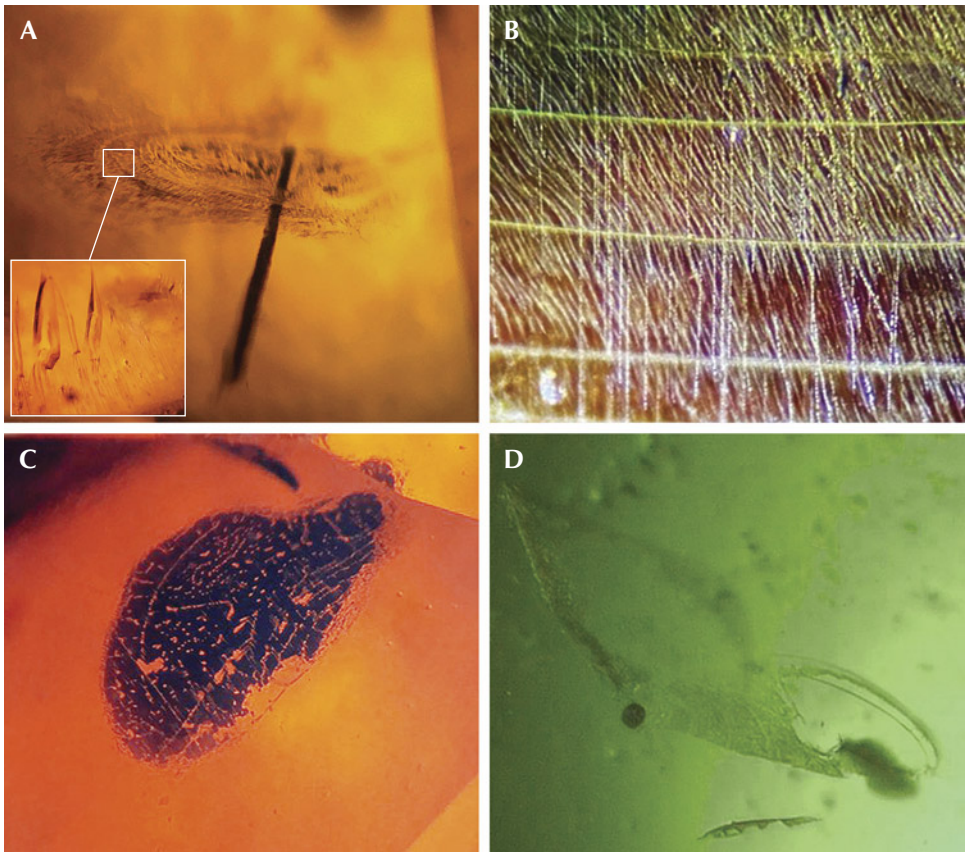

Figure 7. The internal microscopic features of Dong Nai augite. A: In sample A1, a long solid black amphibole inclusion pierces through the center of a fingerprint inclusion resembling a lily pad. B: Sample A4 shows white broken silk-like inclusions of magnetite that cross the twin planes. C and D: Thin films of fingerprint inclusions were commonly found in both green and brown augites (A2 and A11, respectively). Photomicrographs by Le Ngoc Nang; fields of view 4.5 mm (A, C, and D) and 5.5 mm (B).

The hardness of Dong Nai augite was lower than that of other pyroxene gem varieties such as jadeite (7.0–7.5), spodumene (6.5–7.0), and diopside (5.5–6.5). Yet the gemological properties of the green augite were nearly identical to those of chrome diopside, making it difficult to distinguish the two (Anthony et al., 2001).

Internal Features. When examined with a gemological microscope, the 12 cut samples (A1–A12) revealed three types of features: fingerprint inclusions, solid inclusions, and twin planes. The fingerprint inclusions were the most common features, observed as flat roundish or oval shapes and associated with elongate fluid inclusions with pointed tips (figure 7). In one instance, a long solid black acicular inclusion pierced through the center of a fingerprint inclusion resembling a lily pad (figure 7A). This black inclusion was identified as amphibole by Raman analysis. The solid inclusions in figure 7B were broken silk-like crystals that only appeared "white" in reflected light (Bown and Gay, 1959) and were observed only in the brown group. These crystals were aligned in parallel clusters. Raman spectroscopy identified these silk-like crystals as magnetite. Lastly, the twin planes intersected the magnetite crystals (figure 7B).

Chemical Composition and Species. EPMA was used to determine the chemical composition of two of the study samples (A15 and A16). Table 2 reveals some variability for all six oxides: SiO_2 50.64–51.05 wt.%, Al_2O_3 7.88–8.08 wt.%, FeO 5.97–6.33 wt.%, Cr_2O_3 0.010–0.014 wt.%, CaO 15.12–15.74 wt.%, and an unusually high MgO content from 16.69 to 17.22 wt.%. The total alkali ($Na_2O + K_2O$) fell between 1.25 and 1.39 wt.%. There was a much higher amount of sodium than potassium. These oxide concentrations were comparable to the compositions of augite from the state of Montana and Stoffel, Germany (Anthony et al., 2001). In addition, the TiO_2 content of augite from Dong Nai (0.25–0.95 wt.%) was much lower than that of augite from Stoffel (4.33 wt.%) and within range of material from Montana (0.49 wt.%), while the MnO content of Dong Nai augite (0.16–0.19 wt.%) was slightly lower than augite from these other two locations. We noted that the Al_2O_3, MgO, and Na_2O concentrations of Dong Nai augite were much higher than those of augite from Montana and Stoffel, while the opposite was true for CaO concentrations. Based on the measured data in table 2, the percentages of wollastonite (Wo = $Ca_2Si_2O_6$), enstatite (En = $Mg_2Si_2O_6$), and ferrosilite (Fs = $Fe_2Si_2O_6$) in the ternary

TABLE 2. Chemical composition (in wt.%) of six measured points from Dong Nai augite samples A15 and A16.

Chemical composition	A15			A16			Detection limit (wt.%)
	1	2	3	4	5	6	
SiO_2	50.90	50.64	50.95	51.05	50.75	50.87	0.016
TiO_2	0.56	0.59	0.54	0.55	0.52	0.55	0.021
Al_2O_3	8.08	7.88	8.08	7.92	7.92	8.02	0.012
FeO	6.24	5.97	6.16	6.23	6.24	6.33	0.019
MnO	0.10	0.14	0.12	0.16	0.13	0.14	0.017
MgO	16.92	17.2	16.86	17.17	16.69	17.22	0.011
Cr_2O_3	0.010	0.013	0.013	0.011	0.012	0.014	0.010
CaO	15.74	15.59	15.26	15.26	15.12	15.47	0.013
P_2O_5	bdl[a]	0.02	bdl	0.01	0.01	0.03	0.012
Na_2O	1.39	1.28	1.28	1.29	1.25	1.27	0.014
K_2O	bdl	0.01	bdl	bdl	bdl	0.02	0.009
Total	99.93	99.32	99.25	99.64	98.63	99.92	
Atoms per formula unit, 6 O (charge balance)							
Si	1.835	1.835	1.850	1.845	1.856	1.834	—
Ti	0.015	0.016	0.015	0.015	0.014	0.015	—
Al	0.343	0.336	0.346	0.337	0.341	0.341	—
Fe^{3+}	0.052	0.049	0.013	0.030	0.003	0.048	—
Fe^{2+}	0.136	0.132	0.174	0.158	0.187	0.142	—
Mn	0.003	0.004	0.004	0.005	0.004	0.004	—
Mg	0.910	0.929	0.912	0.925	0.910	0.925	—
Cr	0.002	0.003	0.003	0.003	0.003	0.003	—
Ca	0.608	0.605	0.594	0.591	0.592	0.597	—
Na	0.097	0.090	0.090	0.091	0.088	0.089	—
Ternary system (mol. %)							
Wollastonite ($Ca_2Si_2O_6$)	36.8	36.3	35.3	35.3	35.1	35.9	
Enstatite ($Mg_2Si_2O_6$)	55.0	55.8	54.3	55.3	53.9	55.6	
Ferrosilite ($Fe_2Si_2O_6$)	8.2	7.9	10.3	9.4	11.1	8.6	

[a]*bdl = below detection limit*

system were calculated to be 35.1–36.8%, 53.0–55.0%, and 7.9–11.1%, respectively.

Chemical Formula. The elemental concentration data in table 2 show that the cations in the Dong Nai augite can be partitioned among tetrahedral T and octahedral M1 and M2 sites. Morimoto (1989) provides a flow chart for these assignments. Using it, we derive a formula of $(Ca_{0.608}Na_{0.097}Fe^{2+}_{0.038}Mg_{0.254})(Mg_{0.656}Fe^{3+}_{0.053}Fe^{2+}_{0.098}Ti_{0.015}Al_{0.178})(Si_{1.835}Al_{0.165})O_6$ (sample A15, spot 1), similar to the chemical formula of augite from Stoffel, Germany: $(Ca_{0.91}Na_{0.07}Fe^{2+}_{0.04})(Mg_{0.66}Fe^{3+}_{0.13}Fe^{2+}_{0.09}Ti_{0.08}Al_{0.04})(Si_{1.69}Al_{0.31})O_6$ (Anthony et al., 2001). However, the ratio of cations in each site is distributed somewhat differently. At the M2 position, the high amount of Mg^{2+} and low amount of Ca^{2+} in Dong Nai augite are the opposite of the Mg^{2+} and Ca^{2+} content in augite from Stoffel. Secondly, the Al^{3+} content of Dong Nai augite is distributed relatively equally at positions M1 and T, while most of the Al^{3+} in augite from Stoffel is concentrated at position T. The substantial difference in cation distribution at the T, M1, and M2 positions between Dong Nai and Stoffel augites suggests a complicated isomorphic replacement in pyroxene in general and augite in particular, which depends mainly on temperature (Chen et al., 2021).

The concentrations of aluminum and chromium allow augite to be distinguished from chrome diopside. For chrome diopside from the Kola Peninsula in northwestern Russia, the chromium content is higher (0.52–1.45 wt.% Cr_2O_3) and the aluminum content is lower (1.34–3.80 wt.% Al_2O_3) (Zozulya et al., 2009). Similarly, chrome diopside from Schwartzenstein, Austria, shows high chromium content (1.06–1.47 wt.% Cr_2O_3) and low aluminum content (0.07 wt.% Al_2O_3) (Yamaguchi, 1961; Anthony et al., 2001). While chromium is the chromophore for chrome diopside, the chromium content in Dong Nai augite was negligible and could not be the cause of the dark green color. We infer that iron content controls the color in this augite. However, no direct evidence has yet been found, and this will require further study.

X-Ray Diffraction. According to the X-ray diffraction results of brown sample A13 and green sample A14, the main peaks of Dong Nai augite matched those of augite sample 01-080-1864 from the ICSD (Levin, 2018) (figure 8). This confirmed that the studied samples belong to the augite species, a species of monoclinic pyroxene.

Species. Based on chemical composition, the Dong Nai pyroxenes were plotted and classified using the

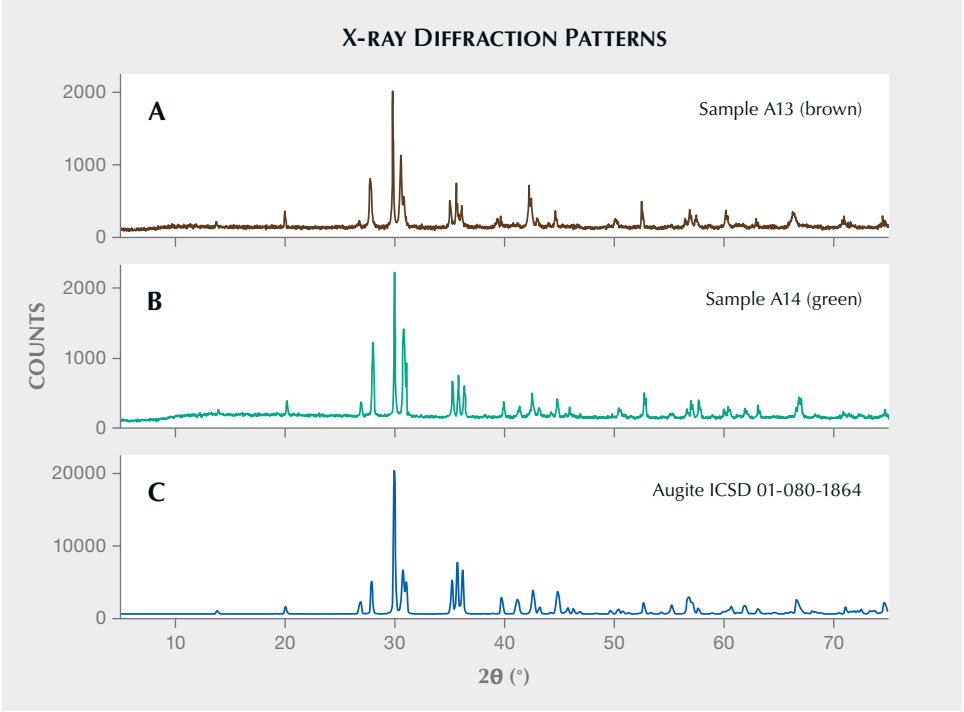

Figure 8. The XRD patterns of augite from Dong Nai (A and B) contain peaks consistent with the pattern of an augite sample from Levin (2018).

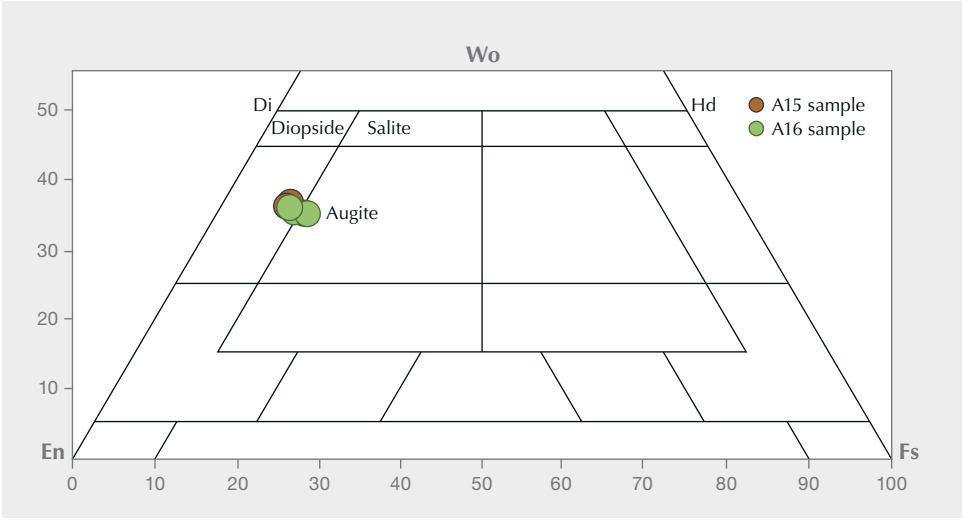

Figure 9. In this classification diagram for quadrilateral pyroxenes, six measured points from samples A15 and A16 (table 2) indicate the zone of magnesium-rich augite (Poldervaart and Hess, 1951).

pyroxene quadrilateral with end members diopside ($CaMgSi_2O_6$ or Di), hedenbergite ($CaFeSi_2O_6$ or Hd), enstatite ($Mg_2Si_2O_6$ or En), and ferrosilite ($Fe_2Si_2O_6$ or Fs) (Poldervaart and Hess, 1951). Wollastonite does not belong to the pyroxenes but to the pyroxenoids, with the formula $Ca_2Si_2O_6$. From table 2, the wollastonite, enstatite, and ferrosilite values were plotted in the pyroxene classification diagram, and the data fell within the augite field (figure 9). Based on Morimoto (1989) and the approval of the Commission on New Minerals and Mineral Names, the Dong Nai pyroxene should be described as magnesium-rich augite.

Raman Spectroscopy. The Raman spectra of the Dong Nai augite samples (brown A1, A2, and A3; green A7, A8, and A9) displayed peaks in the range of 100–1200 cm^{-1} (figure 10), including four vibrational bands assigned to metal-oxygen bond (M-O) stretching and bending (100–400 cm^{-1}), Si-O-Si bending (400–600 cm^{-1}), Si-O_{br} stretching (600–700 cm^{-1}, where O_{br} represents bridging oxygen), and Si-O_{nbr} stretching (700–1200 cm^{-1}, where O_{nbr} represents nonbridging oxygen). The Raman spectra revealed some differences between brown and green augite.

The region from 100 to 400 cm^{-1} exhibited both stretching and bending vibrations of the M-O

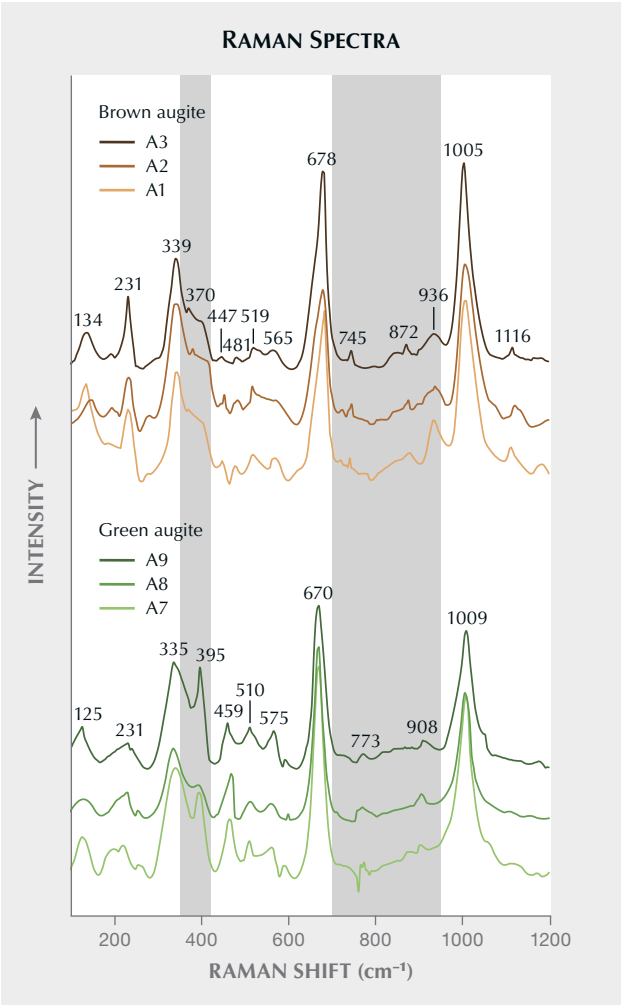

Figure 10. Raman spectra of the two Dong Nai sample groups indicate several differences between green augite (top) and brown augite (bottom) in the ranges of 350–420 cm^{-1} and 700–950 cm^{-1}. Note that a sharp peak at 395 cm^{-1} in the green samples is not observed in the brown samples. In contrast, the peaks at 1116 cm^{-1} and around 872 cm^{-1} are present only in the brown samples. Spectra are offset for clarity.

(Buzatu and Buzgar, 2010; Buzgar et al., 2013). The brown augite group showed peaks around 134, 231, 339, and 370 cm^{-1}, while the green group yielded peaks at 125, 231, 335, and 395 cm^{-1}. We noticed that a strong peak at 395 cm^{-1} was found only in the green augites. Second, the 400–600 cm^{-1} region displayed weak bands at 447, 481, 519, and 565 cm^{-1} for the brown augite, and 459, 510, and 575 cm^{-1} for the green, all related to the bending vibrations of the Si-O group. A peak at 447 cm^{-1} in the brown group was missing in the green samples, whereas other vibrations were similar. Third, a sharp band in the range of 600–700 cm^{-1} is attributed to Si-O_{br} stretching, located at 678 and 670 cm^{-1} for the brown and green samples, respectively. Lastly, the 700–1200 cm^{-1} region is related to Si-O_{nbr} stretching and presented a sharp line around 1005–1009 cm^{-1} for both groups, while the other bands were quite different. In particular, we recorded peaks around 745, 872, 936, and 1116 cm^{-1} for the brown augites and around 773 and 908 cm^{-1} for the green samples. In particular, a peak at 1116 cm^{-1} was well defined in the brown samples but not observed in the green samples. Differences in the 700–1200 cm^{-1} region are typically attributed to the substitution of silicon for aluminum (Buzatu and Buzgar, 2010). In summary, the Raman spectral features of Dong Nai augite displayed the two strongest bands in the 600–700 cm^{-1} range and around 700–1200 cm^{-1}.

The peaks of augite are much stronger in the 700–1000 cm^{-1} region than those of diopside, which only has a peak at 865 cm^{-1} (Buzatu and Buzgar, 2010). Hence, this feature is useful to distinguish augite from diopside when the gemological properties are similar.

CONCLUSIONS

This study has clarified our understanding of the variety and characteristics of augite from Dong Nai Province in Vietnam. The pyroxene xenocrysts from Dong Nai are classified as magnesium-rich augite with the chemical formula $(Ca_{0.608}Na_{0.097}Fe^{2+}_{0.038}Mg_{0.254})(Mg_{0.656}Fe^{3+}_{0.053}Fe^{2+}_{0.098}Ti_{0.015}Al_{0.178})(Si_{1.835}Al_{0.165})O_6$. This material is characterized by its intense dark brown or dark green color, its vitreous luster, and its transparency or translucence. The gemological properties of the green and brown color varieties are identical except for the higher RI and birefringence values for the green samples. The Raman spectra indicate two sharp lines around 1005–1009 cm^{-1}, assigned to Si-O_{nbr} stretching, and 670–678 cm^{-1}, related to Si-O_{br} stretching, along with weaker bands distributed in the 100–1200 cm^{-1} region. Compared with brown augite, the green samples show considerable differences in the 350–400 cm^{-1} range and the 700–950 cm^{-1} range. Augite from Dong Nai has the potential for use in jewelry, particularly as a carving material, and is worthy of further scientific study.

ABOUT THE AUTHORS

Le Ngoc Nang is a postgraduate in the Faculty of Geology at the University of Science, Vietnam National University in Ho Chi Minh City, and CEO of Liu Gemological Research and Application Center (LIULAB). Lam Vinh Phat is manager of gemstone identification, and Pham Minh Tien is a technical specialist, at LIULAB. Dr. Pham Trung Hieu is associate professor and Pham Minh is a lecturer in the Faculty of Geology at the University of Science, Vietnam National University Ho Chi Minh City. Dr. Kenta Kawaguchi is a research fellow in the Faculty of Social and Cultural Studies, Kyushu University in Fukuoka, Japan.

ACKNOWLEDGMENTS

This research was funded by Vietnam National University, Ho Chi Minh City (VNU-HCM) under grant number B2023-18-11. We would also like to express our deep gratitude to Tran Ngoc Vien, who guided us to the study location during our research in the field. We are sincerely thankful to Yasuhiro Shibata of Hiroshima University for technical assistance with EPMA measurements.

REFERENCES

Anthony J.W., Bideaux R.A., Bladh K.W., Nichols M.C., Eds. (2001) *Handbook of Mineralogy*. Mineral Data Publishing, Tucson, Arizona, 813 pp.

Bac D.K., Bao D.V. (2020) Analyzing bio-geo-chemical factors in relation to land use trends on basalt terrain in Dong Nai and nearby areas. *VNU Journal of Science: Earth and Environmental Sciences*, Vol. 36, No. 2, pp. 79–89, http://dx.doi.org/10.25073/2588-1094/vnuees.4542

Bown M.G., Gay P. (1959) The identification of oriented inclusions in pyroxene crystals. *American Mineralogist*, Vol. 44, No 5-6, pp. 592–602.

Buzatu A., Buzgar N. (2010) The Raman study of single-chain silicates. *Analele Ştiintifice de Universitatii "Al. I. Cuza" din Iasi, Seria Geologie*, Vol. 56, No. 1, pp. 107–125.

Buzgar N., Apopei A.I., Diaconu V., Buzatu A. (2013) The composition and source of the raw material of two stone axes of Late

Bronze Age from Neamt County (Romania) - A Raman study. *Analele Ştiintifice de Universitatii "Al. I. Cuza" din Iasi, Seria Geologie*, Vol. 59, No. 1, pp. 5–22.
Chen W., Li Y., La P., Xue Y., Li Z., Xu S., Sheng J. (2021) Influences of thermal treatment temperature on microstructures and properties of glass-ceramics from gold tailings. *Ferroelectrics*, Vol. 579, No. 1, pp. 23–32, http://dx.doi.org/10.1080/00150193.2021.1903264
Co M.C., Hai H.Q. (1994) Report on the result of geological mapping and mineral exploration, Ho Chi Minh City East map series, scale 1:50.000. South Vietnam Geological Mapping Division, General Department of Geology and Minerals of Vietnam [in Vietnamese].
Hurwit K.N. (1988) Gem Trade Lab Notes: Augite, Chinese "onyx." *G&G*, Vol. 24, No. 3, p. 170.
Johnson M.L., McClure S.F., DeGhionno D.G. (1996) Some gemological challenges in identifying black opaque gem materials. *G&G*, Vol. 32, No. 4, pp. 252–261, http://dx.doi.org/10.5741/GEMS.32.4.252
Kawaguchi K., Hayasaka Y., Minh P., Das K., Kimura K. (2022) Origin and tectonic relationship of metagabbro of the Sambagawa Belt, and associated Karasaki mylonites of western Shikoku, Southwest Japan. *Geosciences Journal*, Vol. 26, No. 1, pp. 37–54, http://dx.doi.org/10.1007/s12303-021-0022-6
Levin I. (2018) NIST Inorganic Crystal Structure Database (ICSD), National Institute of Standards and Technology, http://dx.doi.org/10.18434/M32147
Lindsley D.H. (1983) Pyroxene thermometry. *American Mineralogist*, Vol. 68, No. 5-6, pp. 477–493.
Manutchehr-Danai M. (2005) *Dictionary of Gems and Gemology*, 2nd ed. Springer, Berlin, Heidelberg, 1030 pp.
Mei O., Qi L.-J., Hansheng L., Kwok B. (2003) Recent studies on inky black omphacite jade, a new variety of pyroxene jade. *Journal of Gemmology*, Vol. 28, pp. 337–344.
Morimoto N. (1989) Nomenclature of pyroxenes. *Canadian Mineralogist*, Vol. 27, No. 1, pp. 143–156.
O'Donoghue M., Ed. (2006) *Gems: Their Sources, Descriptions, and Identification*, 6th ed. Butterworth-Heinemann, Oxford, UK, 937 pp.
Poldervaart A., Hess H.H. (1951) Pyroxenes in the crystallization of basaltic magma. *Journal of Geology*, Vol. 59, No. 5, pp. 472–489, http://dx.doi.org/10.1086/625891
Son N.D., Du D.C., Hanh D.V., Nam L.D., Phuong H., Phuong D.T., Tue T., Van V.V. (2005) Geological mapping of mineral resource and prospective zoning of Dong Nai Province, scale 1:50.000, Dong Nai Department of Science and Technology [in Vietnamese].
Yamaguchi M. (1961) Chrome-diopsides in the Horoman and Higashi-Akaishi peridotites, Japan. *Memoirs of the Faculty of Science,* Kyūsyū *University. Series D, Geology*, Vol. 10, No. 2, pp. 233–245, http://dx.doi.org/10.5109/1526111
Zozulya D.R., O'Brien H., Peltonen P., Lehtonen M. (2009) Thermobarometry of mantle-derived garnets and pyroxenes of Kola region (NW Russia): Lithosphere composition, thermal regime and diamond prospectivity. *Bulletin of the Geological Society of Finland*, Vol. 81, No. 2, pp. 143–158, http://dx.doi.org/10.17741/bgsf/81.2.003